Journal of Mechanics of Materials and Structures

IMPROVED THERMOELASTIC COEFFICIENTS OF A NOVEL SHORT FUZZY FIBER-REINFORCED COMPOSITE WITH WAVY CARBON NANOTUBES

Shailesh I. Kundalwal and Manas C. Ray

Volume 9, No. 1 January 2014

msp

JOURNAL OF MECHANICS OF MATERIALS AND STRUCTURES
Vol. 9, No. 1, 2014
dx.doi.org/10.2140/jomms.2014.9.1

IMPROVED THERMOELASTIC COEFFICIENTS OF A NOVEL SHORT FUZZY FIBER-REINFORCED COMPOSITE WITH WAVY CARBON NANOTUBES

SHAILESH I. KUNDALWAL AND MANAS C. RAY

The elastic response of a novel short fuzzy fiber-reinforced composite (SFFRC) has recently been investigated by the authors (*Mech. Mater.* **53** (2012), 47–60). The distinctive feature of the construction of this novel SFFRC is that straight carbon nanotubes (CNTs) are radially grown on the circumferential surfaces of unidirectional short carbon fiber reinforcements. The waviness of CNTs is intrinsic to many manufacturing processes and plays an important role in the thermomechanical behavior of CNT-reinforced composites. However, the effect of the waviness of CNTs on the thermoelastic response of a SFFRC has yet to be investigated. Therefore, we investigate the effect of wavy CNTs on the thermoelastic properties of this SFFRC, revealing that the axial thermoelastic coefficients of the SFFRC significantly increase when the wavy CNTs are coplanar with the longitudinal plane of the carbon fibers for higher values of the waviness factor and wave frequency of the CNTs. The effective values of the thermal expansion coefficients of this SFFRC are also found to be sensitive to change in temperature.

A list of abbreviations and symbols can be found starting on page 21.

1. Introduction

Research on the synthesis of molecular carbon structures by an arc-discharge method for the evaporation of carbon led to the discovery of an extremely thin, needle-like graphitic carbon nanotube (CNT) [Iijima 1991]. Researchers probably thought that CNTs might be useful as nanoscale fibers for developing novel CNT-reinforced nanocomposites, and this conjecture motivated them to accurately study the physical properties (mechanical, thermal, and electrical) of CNTs. Numerous experimental and numerical studies revealed that the axial Young's modulus of CNTs is in the terapascal range [Treacy et al. 1996; Natsuki et al. 2004; Shen and Li 2004; Liu et al. 2005; Li and Guo 2008]. The quest for utilizing these exceptional mechanical properties of CNTs and their high aspect ratio led to the emergence of a new area of research on the development of CNT-reinforced nanocomposites [Odegard et al. 2003; Ashrafi and Hubert 2006; Seidel and Lagoudas 2006; Esteva and Spanos 2009; Ray and Batra 2009; Meguid et al. 2010; Khondaker and Keng 2012].

As nanoscale graphite structures, CNTs are of great interest not only for their mechanical properties but also for their thermal properties. For example, in several studies [Bandow 1997; Yosida 2000; Maniwa et al. 2001] the coefficients of thermal expansion (CTEs) of CNTs and their bundles are determined by using X-ray diffraction techniques. Bandow [1997] found that the CTE in the radial direction of multiwalled CNTs (MWCNTs) is almost the same as the CTE of graphite. Yosida [2000] and Maniwa

Keywords: short fuzzy fiber composite, wavy CNTs, micromechanics, thermoelastic coefficients.

et al. [2001] estimated the CTEs of single-walled CNT (SWCNT) bundles. Their results indicate that CNT bundles have a negative CTE at low temperatures and a positive CTE at high temperatures. Raravikar et al. [2002] estimated the CTEs of armchair (5, 5) and (10, 10) SWCNTs by using a molecular dynamics simulation (MDS) and found that the CTE of the CNT in the radial direction is less than that in the axial direction. Jiang et al. [2004] presented an analytical method to determine the CTEs of SWCNTs based on the interatomic potential and the local harmonic model. They found that all CTEs of SWCNTs are negative at low and room temperatures, and become positive at high temperatures. Kwon et al. [2004] performed a MDS and reported that the axial and radial CTEs of CNTs are nonlinear functions of change in temperature. Kirtania and Chakraborty [2009] presented a finite element (FE) analysis to estimate the CTEs of SWCNTs and demonstrated that the CTEs of SWCNTs increase uniformly with increase in the diameter of the SWCNT. The nonequilibrium Green's function method was employed by Jiang et al. [2009] to investigate the CTEs of SWCNTs and graphene. They found that the axial CTE is positive in the whole temperature range while the radial CTE is negative at low temperatures. Alamusi et al. [2012] investigated the axial CTEs of SWCNTs and MWCNTs by using a MDS, considering the effects of temperature and CNT diameter. For all CNTs, the obtained results revealed that axial CTEs are negative within a wide low-temperature range and positive in a high temperature range, and the temperature range for negative axial CTEs narrows as the diameter of the CNT decreases. Extensive research has also been carried out concerning the prediction of the CTEs of CNT-reinforced composites [Pipes and Hubert 2003; Kirtania and Chakraborty 2009]. In these studies, the results indicate that the addition of CNTs into the matrix causes significant improvement in the thermoelastic response of the CNT-reinforced composite as compared to that of the base composite.

It has been reported in many experimental studies [Shaffer and Windle 1999; Qian et al. 2000; Zhang et al. 2008; Yamamoto et al. 2009; Tsai et al. 2011] that CNTs are actually curved cylindrical tubes. The use of long CNTs in CNT-reinforced nanocomposites has revealed that CNT curvature significantly reduces the effective properties of the CNT-reinforced composite [Fisher et al. 2002; Berhan et al. 2004; Shi et al. 2004; Anumandla and Gibson 2006]. The effect of CNT curvature on the polymer matrix nanocomposite stiffness has been investigated by Pantano and Cappello [2008]. They concluded that in the presence of weak bonding, enhancement of the nanocomposite stiffness can be achieved through the bending energy of CNTs rather than through their axial stiffness. Li and Chou [2009] studied the failure of CNT/polymer matrix composites by using a micromechanics model and conducting FE simulations. They found that CNT waviness tends to reduce the elastic modulus and tensile strength of the nanocomposite but increases its ultimate strain. Farsadi et al. [2013] developed a three-dimensional FE model to investigate the influence of the waviness of the CNTs on the elastic moduli of a CNT-reinforced composite.

In addition to the waviness of CNTs, significant technical and manufacturing challenges have hindered the development of large-scale CNT-enhanced structures [Ajayan and Tour 2007; Schulte and Windle 2007]. Alignment, dispersion, and adhesion of CNTs in polymer matrices are vital for structural composite applications [Thostenson et al. 2001; Ajayan and Tour 2007; Schulte and Windle 2007]. More success can be achieved in improving the transverse multifunctional properties of hybrid CNT-reinforced composites by growing short CNTs on the circumferential surfaces of advanced fibers [Bower et al. 2000; Veedu et al. 2006; Qiu et al. 2007; Garcia et al. 2008]. For example, Veedu et al. [2006] developed a multifunctional composite in which CNTs are grown on the circumferential surfaces of the fibers and found that the presence of CNTs on the surfaces of the fibers reduces the effective CTE

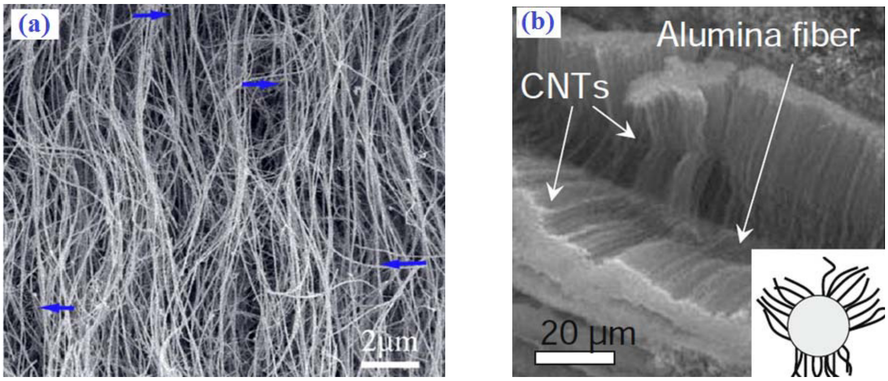

Figure 1. Left: SEM image of vertically aligned curved CNTs (adapted with permission from [Zhang et al. 2008]). Right: SEM image of aligned CNTs grown on alumina fiber (adapted with permission from [Yamamoto et al. 2009]).

of the multifunctional composite up to 62% compared to that of the base composite (that is, without CNTs). Qiu et al. [2007] developed a multifunctional composite through an effective infiltration-based vacuum-assisted resin transfer moulding process. Their study indicated that the effective CTE of the multifunctional composite was reduced up to 25.2% compared with that of the composite without CNTs. A fiber coated with radially grown CNTs on its circumferential surface is called a "fuzzy fiber" [Garcia et al. 2008; Yamamoto et al. 2009; Chatzigeorgiou et al. 2012], and the resulting composite may be called a fuzzy fiber-reinforced composite (FFRC). Chatzigeorgiou et al. [2012] estimated the thermoelastic properties of fuzzy fiber composites in which a carbon fiber is coated with radially aligned straight CNTs by employing the asymptotic expansion homogenization method. They reported that the radial CTE of the fuzzy fiber composite is one order of magnitude less than its axial CTE. Recently, the elastic properties and the load transfer characteristics of a novel short fuzzy fiber-reinforced composite (SFFRC) have been extensively studied in [Kundalwal and Ray 2012; Kundalwal 2013].

Scanning electron microscopy (SEM) images analyzed in [Zhang et al. 2008] and [Yamamoto et al. 2009] are shown in Figure 1. They show clearly that CNTs remain highly curved when they are grown on the surfaces of advanced fibers. It is hypothesized that their affinity to becoming curved is due to their high aspect ratio and associated low bending stiffness. Since the addition of CNTs in hybrid CNT-reinforced composites influences the thermoelastic properties of the hybrid nanocomposites, the waviness of the CNTs may also affect the effective thermoelastic response of the SFFRC. However, the thermoelastic response of such a hybrid nanocomposite, being composed of short fuzzy fiber reinforcements coated with wavy CNTs, has not yet been investigated. Therefore, in this study we have endeavored to investigate the effect of waviness of CNTs on the effective thermoelastic properties of a SFFRC.

The outline is as follows: Section 2 briefly describes the architecture of the SFFRC containing wavy CNTs coplanar with either of the two mutually orthogonal planes. Section 3 presents the development of the Mori–Tanaka (MT) models for estimating the effective thermoelastic properties of the SFFRC and its constituent phases. In Section 4, numerical results are presented. Finally, Section 5 delineates the conclusions drawn from this study.

2. Architecture of a novel SFFRC

The top part of Figure 2 represents a lamina of a SFFRC in which the short fuzzy fibers are uniformly reinforced in the polymer matrix. Its in-plane cross section is illustrated in Figure 2, bottom. The short fuzzy fiber coated with sinusoidally wavy CNTs [Fisher et al. 2002; Berhan et al. 2004; Anumandla and Gibson 2006; Pantano and Cappello 2008; Zhang et al. 2008; Tsai et al. 2011; Farsadi et al. 2013] reinforced in the polymer matrix can be viewed as a circular cylindrical short composite fuzzy fiber (SCFF), as illustrated in Figure 3. The SCFFs are assumed to be uniformly dispersed over the volume of a lamina of the SFFRC in such a way that the three orthogonal principal material coordinate axes (1-2-3) exist in the composite as shown in Figure 2, top. The architecture of the representative volume element

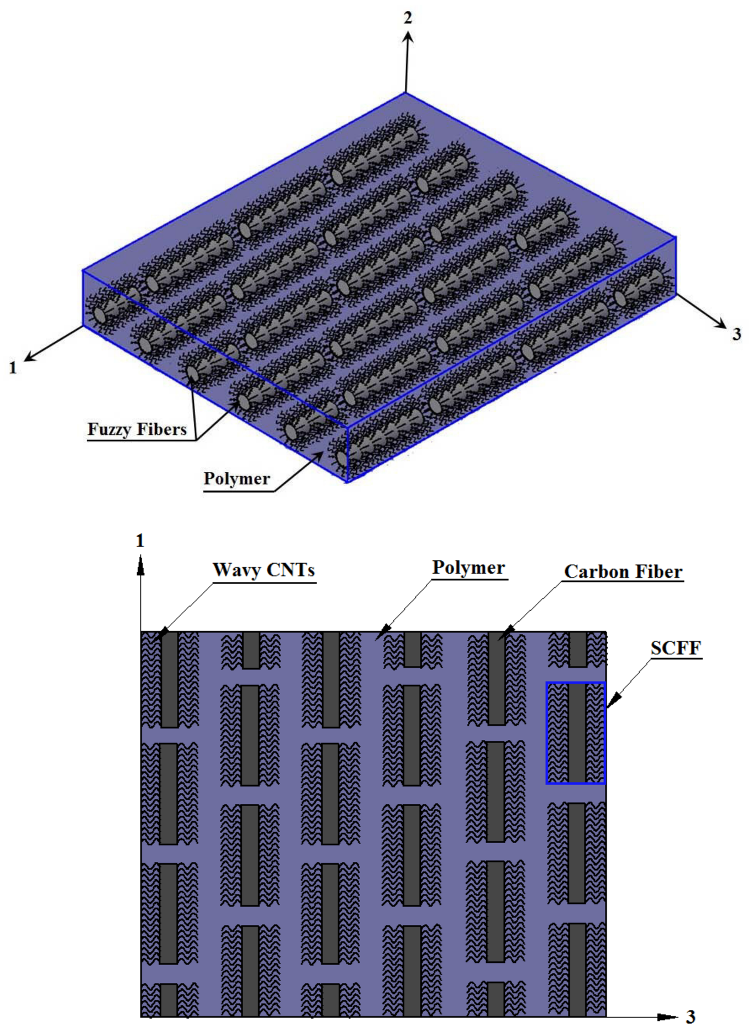

Figure 2. Top: schematic diagram of a lamina made of the SFFRC containing wavy CNTs. Bottom: In-plane cross section of the SFFRC lamina. (Wavy CNTs are coplanar with the longitudinal plane of the carbon fiber.)

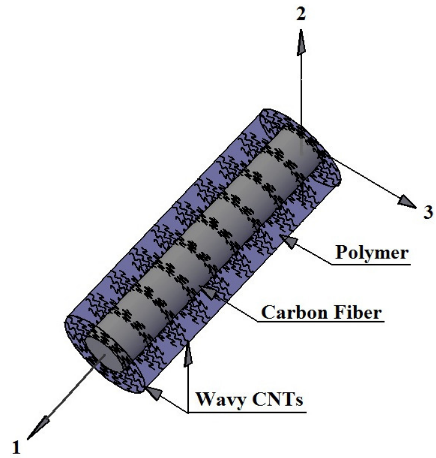

Figure 3. Fuzzy fiber coated with wavy CNTs reinforced in the polymer matrix (wavy CNTs are coplanar with the transverse plane of the carbon fiber).

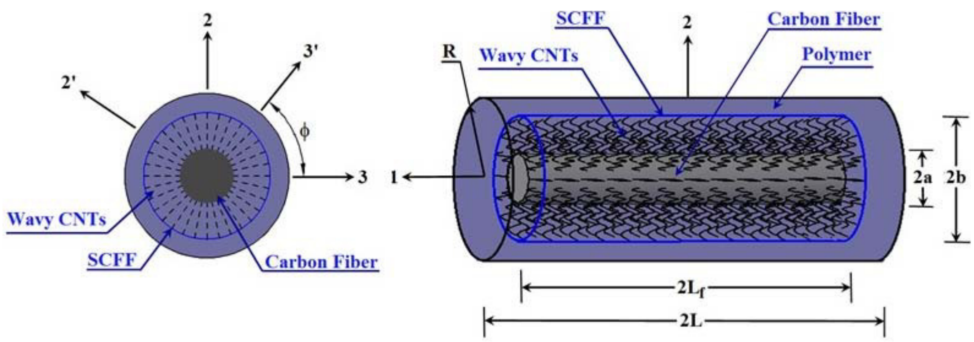

Figure 4. Architecture of the RVE of the SFFRC in which the SCFF is embedded in the polymer material.

(RVE) of the SFFRC in which the SCFF embedded in the polymer material is schematically illustrated in Figure 4. The orientation of the plane of the wavy CNTs radially grown on the circumferential surface of the carbon fiber is an important issue because the planar orientations of the wavy CNTs may influence the thermoelastic properties of the SFFRC; this issue needs to be carefully addressed. Two possible planar orientations of the wavy CNTs are considered herein. The wavy CNTs are coplanar with either the longitudinal (that is, the 1-3 or $1'$-$3'$) or the transverse (that is, the 2-3 or $2'$-$3'$) plane of the carbon fiber, as shown in Figures 2 and 3, respectively. Investigation of the effect of all other planar orientations of the wavy CNTs is beyond the scope of the present study.

3. Modeling of the effective thermoelastic properties of a novel SFFRC and its constituent phases

This section deals with the procedures of employing the MT model to predict the effective thermoelastic properties of the SFFRC and its constituent phases. The various steps involved in the computation of the effective thermoelastic properties of the SFFRC are outlined as follows.

- The first step in modeling the SFFRC is to determine the effective thermoelastic properties of a polymer matrix nanocomposite (PMNC) containing wavy CNTs coplanar with either the longitudinal (that is, the 1-3 or $1'$-$3'$) or the transverse (that is, the 2-3 or $2'$-$3'$) plane of the carbon fiber.
- Subsequently, considering the PMNC material as the matrix phase and the short carbon fibers as the reinforcement, the effective thermoelastic properties of the SCFF can be computed.
- Finally, using the effective thermoelastic properties of the SCFF and the polymer matrix, the effective thermoelastic properties of the SFFRC can be obtained.

3.1. ***Effective thermoelastic properties of the PMNC.*** From the constructional features of the SCFF, it may be seen that the carbon fiber is wrapped by a lamina of PMNC material, as illustrated in Figure 5. The average effective thermoelastic properties of the annular portion of the PMNC material surrounding the carbon fiber can be approximated by estimating the effective thermoelastic properties of the unwound lamina containing wavy CNTs. Hence, the effective elastic coefficient matrix $[\overline{C}^{\mathrm{NC}}]$ and the effective thermal expansion coefficient vector $\{\overline{\alpha}^{\mathrm{NC}}\}$ of the unwound lamina containing wavy CNTs are to be estimated a priori. Subsequently, appropriate transformations and homogenization procedures can be

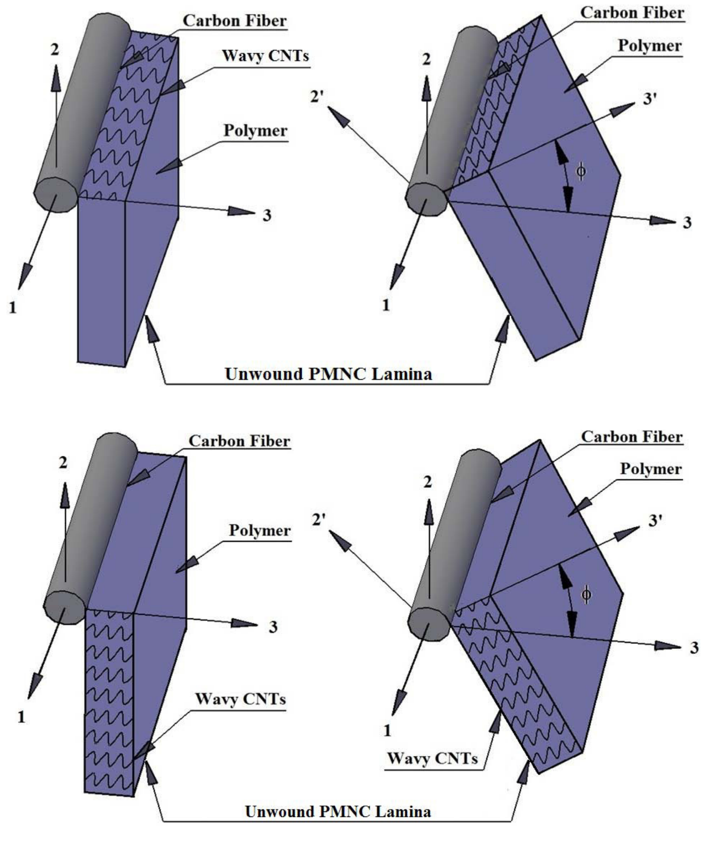

Figure 5. Unwound lamina of PMNC containing wavy CNTs coplanar with the longitudinal (top) or transverse (bottom) plane of the carbon fiber.

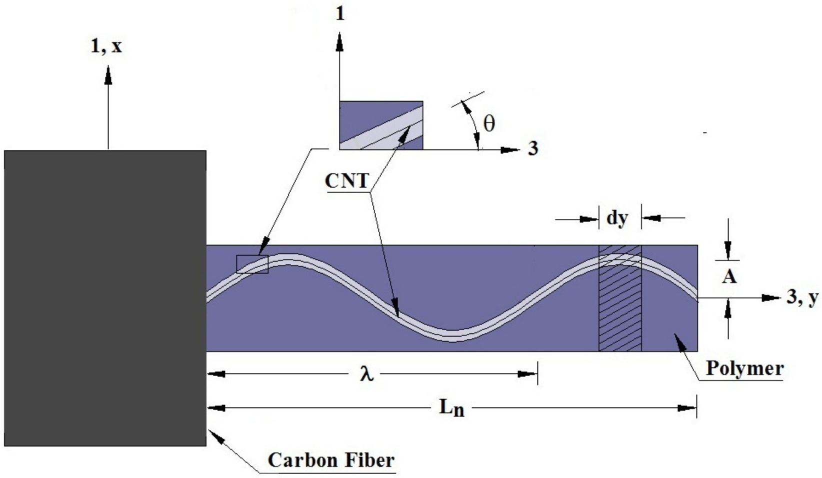

Figure 6. RVE of unwound PMNC material containing a wavy CNT coplanar with the longitudinal (that is, 1-3) plane of the carbon fiber (adapted with permission from [Kundalwal and Ray 2013]).

carried out on $[\overline{\overline{C}}^{\mathrm{NC}}]$ and $\{\overline{\alpha}^{\mathrm{NC}}\}$ to determine the effective thermoelastic properties of the annular portion of PMNC surrounding the carbon fiber.

Wavy CNTs coplanar with the longitudinal plane of the carbon fiber. We first consider the wavy CNTs to be coplanar with the longitudinal plane (the 1-3 or $1'$-$3'$ plane) of the carbon fiber, as shown in Figures 2 and 4, while computing the thermoelastic properties of the PMNC. An appropriate RVE of unwound PMNC material containing a wavy CNT can be considered to investigate the thermoelastic properties of the unwound PMNC material. Such an RVE is schematically illustrated in Figure 6. The RVE shown in Figure 6 can be divided into infinitesimally thin slices of thickness dy and each slice can be treated as an off-axis unidirectional lamina in which the CNT axis makes an angle θ with the radial direction. The CNT waviness is assumed to be sinusoidal in the longitudinal plane of the carbon fiber and is defined by

$$x = A\sin(\omega y), \quad \omega = n\pi/L_n, \tag{1}$$

in which A and L_n are the amplitude of the CNT wave and the linear distance between the CNT ends, respectively, and n represents the number of CNT waves. The running length, L_{nr}, of the CNT is given by

$$L_{nr} = \int_0^{L_n} \sqrt{1 + A^2\omega^2\cos^2(\omega y)}\, dy, \tag{2}$$

where the angle θ shown in Figure 6 is given by

$$\tan\theta = dx/dy = A\omega\cos(\omega y). \tag{3}$$

The effective thermoelastic properties at any point of any slice of the unwound lamina of PMNC containing sinusoidally wavy CNTs where the CNT axis makes an angle θ with the radial direction (3 or $3'$) can be approximated by transforming the effective thermoelastic properties of the unwound lamina of PMNC containing straight CNTs. Hence, in what follows the MT model for predicting the effective thermoelastic properties of the unwound lamina of PMNC with straight CNTs will be presented first. Due to difficulties in the atomistic modeling of CNTs inside the polymer matrix environment, researchers have considered CNTs as equivalent solid fibers for estimating the effective thermoelastic properties of CNT-reinforced composites [Fisher et al. 2002; Pipes and Hubert 2003; Berhan et al. 2004; Anumandla and Gibson 2006; Pantano and Cappello 2008; Tsai et al. 2011; Farsadi et al. 2013]. Thus, considering CNTs as solid fibers, the MT model [Mori and Tanaka 1973] can be utilized to estimate the effective elastic coefficient matrix $[C^{nc}]$ of the unwound lamina of PMNC with straight CNTs [Benveniste 1987]:

$$[C^{nc}] = [C^p] + v_n([C^n] - [C^p])([\tilde{A}_1][v_p[I] + v_n[\tilde{A}_1]]^{-1}), \tag{4}$$

in which

$$[\tilde{A}_1] = \big[[I] + [S^n]([C^p])^{-1}([C^n] - [C^p])\big]^{-1},$$

where v_n and v_p represent the volume fractions of the CNT fiber and polymer material, respectively, present in the RVE of the PMNC. The square matrix $[S^n]$ represents the Eshelby tensor for the cylindrical CNT. The elements of the Eshelby tensor $[S^n]$ for the cylindrical CNT reinforcement in the isotropic polymer matrix are explicitly written as [Qiu and Weng 1990]

$$[S^n] = \begin{bmatrix} S^n_{1111} & S^n_{1122} & S^n_{1133} & 0 & 0 & 0 \\ S^n_{2211} & S^n_{2222} & S^n_{2233} & 0 & 0 & 0 \\ S^n_{3311} & S^n_{3322} & S^n_{3333} & 0 & 0 & 0 \\ 0 & 0 & 0 & S^n_{2323} & 0 & 0 \\ 0 & 0 & 0 & 0 & S^n_{1313} & 0 \\ 0 & 0 & 0 & 0 & 0 & S^n_{1212} \end{bmatrix}, \tag{5}$$

in which

$$S^n_{1111} = S^n_{2222} = \frac{5 - 4\nu^p}{8(1 - \nu^p)}, \quad S^n_{3333} = 0, \quad S^n_{1122} = S^n_{2211} = \frac{4\nu^p - 1}{8(1 - \nu^i)},$$
$$S^n_{1133} = S^n_{2233} = \frac{\nu^p}{2(1 - \nu^p)}, \quad S^n_{3311} = S^n_{3322} = 0, \quad S^n_{1313} = S^n_{2323} = 1/4, \quad S^n_{1212} = \frac{3 - 4\nu^p}{8(1 - \nu^p)},$$

where ν^p denotes the Poisson's ratio of the polymer matrix.

Using the effective elastic coefficient matrix $[C^{nc}]$, the effective thermal expansion coefficient vector $\{\alpha^{nc}\}$ for unwound PMNC with straight CNTs can be derived in the form of [Laws 1973] as

$$\{\alpha^{nc}\} = \{\alpha^n\} + ([C^{nc}]^{-1} - [C^n]^{-1})([C^n]^{-1} - [C^p]^{-1})^{-1}(\{\alpha^n\} - \{\alpha^p\}), \tag{6}$$

where $\{\alpha^n\}$ and $\{\alpha^p\}$ are the thermal expansion coefficient vectors of the CNT fiber and the polymer material, respectively. The effective elastic coefficient matrix $[C^{\mathrm{NC}}]$ and the effective thermal expansion coefficient vector $\{\alpha^{\mathrm{NC}}\}$ at any point of any slice of the unwound lamina of PMNC where the CNT is inclined at an angle θ with the 3 (3′)-axis can be derived by employing the appropriate transformations:

$$[C^{\mathrm{NC}}] = [T_1]^{-T}[C^{nc}][T_1]^{-1}, \quad \{\alpha^{\mathrm{NC}}\} = [T_1]^{-T}\{\alpha^{nc}\}, \tag{7}$$

in which

$$[T_1] = \begin{bmatrix} k^2 & 0 & l^2 & 0 & kl & 0 \\ 0 & 1 & 0 & 0 & 0 & 0 \\ l^2 & 0 & k^2 & 0 & -kl & 0 \\ 0 & 0 & 0 & k & 0 & -l \\ -2kl & 0 & 2kl & 0 & k^2-l^2 & -n \\ 0 & 0 & 0 & l & 0 & k \end{bmatrix},$$

with

$$k = \cos\theta = [1 + \{n\pi A/L_n \cos(n\pi y/L_n)\}^2]^{-1/2}$$

and

$$l = \sin\theta = n\pi A/L_n \cos(n\pi y/L_n)[1 + \{n\pi A/L_n \cos(n\pi y/L_n)\}^2]^{-1/2}.$$

Subsequently, the average effective elastic coefficient matrix $[\overline{C}^{\mathrm{NC}}]$ and the thermal expansion coefficient vector $\{\overline{\alpha}^{nc}\}$ of the lamina of unwound PMNC material containing wavy CNTs can be obtained by averaging the transformed elastic coefficients (C_{ij}^{NC}) and the thermal expansion coefficients ($\alpha_{ij}^{\mathrm{NC}}$) over the linear distance between the CNT ends as [Hsiao and Daniel 1996]

$$[\overline{C}^{\mathrm{NC}}] = \frac{1}{L_n}\int_0^{L_n} [C^{\mathrm{NC}}]\,dy, \quad \{\overline{\alpha}^{\mathrm{NC}}\} = \frac{1}{L_n}\int_0^{L_n} \{\alpha^{\mathrm{NC}}\}\,dy. \tag{8}$$

When the carbon fiber is viewed to be wrapped by such an unwound lamina of PMNC, the matrix $[\overline{C}^{\mathrm{NC}}]$ and the vector $\{\overline{\alpha}^{\mathrm{NC}}\}$ as given by (8) also provide the effective properties at a point located in the PMNC with respect to the $1'$-$2'$-$3'$ coordinate system, where the wavy CNT is grown at an orientation angle ϕ with the 3-axis in the 2-3 plane as shown in Figures 4 and 5. Hence, at any point in the PMNC surrounding the carbon fiber, the effective elastic coefficient matrix $[\overline{C}^{\mathrm{PMNC}}]$ and the effective thermal expansion coefficient vector $\{\overline{\alpha}^{\mathrm{PMNC}}\}$ of the PMNC with respect to the 1-2-3 coordinate system turn out to be dependent on the CNT orientation angle ϕ and can be determined by the following transformations:

$$[\overline{C}^{\mathrm{PMNC}}] = [T]^{-T}[\overline{C}^{\mathrm{NC}}][T]^{-1}, \quad \{\overline{\alpha}^{\mathrm{PMNC}}\} = [T]^{-T}\{\overline{\alpha}^{\mathrm{NC}}\}, \tag{9}$$

where

$$[T] = \begin{bmatrix} 1 & 0 & 0 & 0 & 0 & 0 \\ 0 & m^2 & n^2 & mn & 0 & 0 \\ 0 & n^2 & m^2 & -mn & 0 & 0 \\ 0 & -2mn & 2mn & m^2-n^2 & 0 & 0 \\ 0 & 0 & 0 & 0 & m & -n \\ 0 & 0 & 0 & 0 & n & m \end{bmatrix}, \quad \text{with } m = \cos\phi \text{ and } n = \sin\phi.$$

From (9) it is obvious that the effective thermoelastic properties at any point in the PMNC surrounding the carbon fiber with respect to the principle material coordinate axes of the SFFRC vary over the annular cross section of the PMNC phase of the RVE of the SCFF. However, without loss of generality, it may be considered that the volume average of these effective thermoelastic properties over the volume of the PMNC can be treated as the constant effective elastic coefficient matrix $[C^{\mathrm{PMNC}}]$ and the constant effective thermal expansion coefficient vector $\{\alpha^{\mathrm{PMNC}}\}$ of PMNC containing sinusoidally wavy CNTs surrounding the carbon fiber with respect to the 1-2-3 coordinate axes of the SFFRC. These are given by

$$
\begin{aligned}
[C^{\text{PMNC}}] &= \frac{1}{\pi(b^2-a^2)} \int_0^{2\pi}\int_a^b [\overline{C}^{\text{PMNC}}] r\, dr\, d\phi, \\
\{\alpha^{\text{PMNC}}\} &= \frac{1}{\pi(b^2-a^2)} \int_0^{2\pi}\int_a^b \{\overline{\alpha}^{\text{PMNC}}\} r\, dr\, d\phi.
\end{aligned} \tag{10}
$$

Thus the effective constitutive relations for the PMNC material surrounding the carbon fiber with respect to the principle material coordinate (1-2-3) axes of the SFFRC can be expressed as

$$
\{\sigma^{\text{PMNC}}\} = [C^{\text{PMNC}}](\{\epsilon^{\text{PMNC}}\} - \{\alpha^{\text{PMNC}}\}\Delta T), \tag{11}
$$

in which ΔT represents the temperature deviation from a reference temperature.

Wavy CNTs coplanar with the transverse plane of the carbon fiber. Now the CNT waviness is assumed to be sinusoidal in the transverse plane (2-3 or 2′-3′) of the carbon fiber, as shown in Figure 3, and is characterized by

$$
z = A\sin(\omega y), \quad \omega = n\pi/L_n, \tag{12}
$$

in which the angle θ shown in Figure 7 is given by

$$
\tan\theta = dz/dy = A\omega\cos(\omega y). \tag{13}
$$

The procedure of utilizing the MT model presented in Section 3.1 for determining the effective thermoelastic properties of the unwound lamina of PMNC with straight CNTs can be utilized to estimate the effective thermoelastic properties of the unwound lamina of PMNC with wavy CNTs coplanar with the transverse plane of the carbon fiber. Once $[C^{nc}]$ and $\{\alpha^{nc}\}$ are computed by (4) and (6), respectively, the effective elastic coefficient matrix $[C^{\text{NC}}]$ and the effective thermal expansion coefficient vector $\{\alpha^{\text{NC}}\}$ at any point of any slice of the unwound lamina of PMNC where the CNT is inclined at an angle θ with the 3 (3′)-axis can be derived by employing the appropriate transformations for the wavy CNTs coplanar with the transverse plane of the carbon fiber:

$$
[C^{\text{NC}}] = [T_2]^{-T}[C^{nc}][T_2]^{-1}, \quad \{\alpha^{\text{NC}}\} = [T_2]^{-T}\{\alpha^{nc}\}, \tag{14}
$$

in which

$$
[T_2] = \begin{bmatrix} 1 & 0 & 0 & 0 & 0 & 0 \\ 0 & k^2 & l^2 & kl & 0 & 0 \\ 0 & l^2 & k^2 & -kl & 0 & 0 \\ 0 & -2kl & 2kl & k^2-l^2 & 0 & 0 \\ 0 & 0 & 0 & 0 & k & -l \\ 0 & 0 & 0 & 0 & l & k \end{bmatrix}.
$$

Subsequently, (8) and (10) can be used to estimate the effective elastic coefficient matrix $[C^{\text{PMNC}}]$ and thermal expansion coefficient vector $\{\alpha^{\text{PMNC}}\}$ of the PMNC material surrounding the carbon fiber when the wavy CNTs are coplanar with the transverse plane of the carbon fiber.

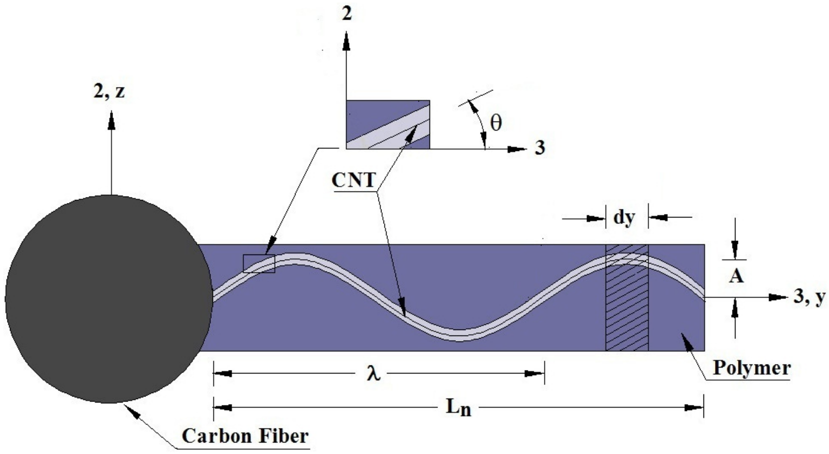

Figure 7. RVE of the unwound PMNC material containing a wavy CNT to be coplanar with the transverse plane (that is, 2-3 plane) of the carbon fiber (adapted with permission from [Kundalwal and Ray 2013]).

3.2. ***Effective thermoelastic properties of the SCFF.*** The second step in modeling the SFFRC is to estimate the effective thermoelastic properties of the SCFF. Utilizing the effective elastic properties of PMNC containing wavy CNTs derived in the previous section as the matrix material properties and with the carbon fiber aligned along the 1-direction as the reinforcement, the MT model presented for the unwound PMNC can be augmented to derive the effective elastic coefficient matrix $[C^{\mathrm{SCFF}}]$ of a lamina made of the SCFF:

$$[C^{\mathrm{SCFF}}] = [C^{\mathrm{PMNC}}] + \bar{v}_f([C^f] - [C^{\mathrm{PMNC}}])([\tilde{A}_2][v_{\mathrm{PMNC}}[I] + v_f[\tilde{A}_2]]^{-1}), \tag{15}$$

where

$$[\tilde{A}_2] = \big[[I] + [S_f]([C^{\mathrm{PMNC}}])^{-1}([C^f] - [C^{\mathrm{PMNC}}])\big]^{-1},$$

and where $\bar{v}_f$ and v_{PMNC} are the volume fractions of the carbon fiber and PMNC, respectively, with respect to the volume of the RVE of the SCFF, and the Eshelby tensor, $[S^f]$, is determined based on the elastic properties of the PMNC and the shape of the carbon fiber. It should be noted that the PMNC material is transversely isotropic and, consequently, the Eshelby tensor [Li and Dunn 1998] corresponding to transversely isotropic material is utilized to compute the matrix $[S^f]$. The elements of the Eshelby tensor for the cylindrical carbon fiber embedded in the transversely isotropic PMNC material are explicitly given by [Li and Dunn 1998]:

$$[S^f] = \begin{bmatrix} S^f_{1111} & S^f_{1122} & S^f_{1133} & 0 & 0 & 0 \\ S^f_{2211} & S^f_{2222} & S^f_{2233} & 0 & 0 & 0 \\ S^f_{3311} & S^f_{3322} & S^f_{3333} & 0 & 0 & 0 \\ 0 & 0 & 0 & S^f_{2323} & 0 & 0 \\ 0 & 0 & 0 & 0 & S^f_{1313} & 0 \\ 0 & 0 & 0 & 0 & 0 & S^f_{1212} \end{bmatrix}, \tag{16}$$

in which

$$S^f_{1111} = S^f_{2222} = \frac{5C_{11}^{\text{PMNC}} + C_{12}^{\text{PMNC}}}{8C_{11}^{\text{PMNC}}}, \quad S^f_{1122} = S^f_{2211} = \frac{3C_{12}^{\text{PMNC}} - C_{11}^{\text{PMNC}}}{8C_{11}^{\text{PMNC}}}, \quad S^f_{1133} = S^f_{2233} = \frac{C_{13}^{\text{PMNC}}}{2C_{11}^{\text{PMNC}}},$$

$$S^f_{3311} = S^f_{3322} = 0, \quad S^f_{1313} = S^f_{2323} = 1/4, \quad S^f_{3333} = 0, \quad S^f_{1212} = \frac{3C_{11}^{\text{PMNC}} - C_{12}^{\text{PMNC}}}{8C_{11}^{\text{PMNC}}}.$$

Using the effective elastic coefficient matrix $[C^{\text{SCFF}}]$, the effective thermal expansion coefficient vector $\{\alpha^{\text{SCFF}}\}$ for the SCFF can be determined as follows [Laws 1973]:

$$\{\alpha^{\text{SCFF}}\} = \{\alpha^f\} + ([C^{\text{SCFF}}]^{-1} - [C^f]^{-1})([C^f]^{-1} - [C^{\text{PMNC}}]^{-1})^{-1}(\{\alpha^f\} - \{\alpha^{\text{PMNC}}\}), \tag{17}$$

where $[C^f]$ and $\{\alpha^f\}$ are the elastic coefficient matrix and thermal expansion coefficient vector of the carbon fiber, respectively.

3.3. ***Effective thermoelastic properties of the SFFRC.*** Considering the SCFF as the cylindrical reinforcement embedded in the isotropic polymer matrix, the effective elastic properties $[C]$ of the SFFRC can be determined by utilizing the MT model as follows:

$$[C] = [C^p] + v_{\text{SCFF}}([C^{\text{SCFF}}] - [C^p])\big([\tilde{A}_3]\big[\bar{v}_P[I] + v_{\text{SCFF}}[\tilde{A}_3]\big]^{-1}\big), \tag{18}$$

in which

$$[\tilde{A}_3] = \big[[I] + [S^{\text{SCFF}}]([C^p])^{-1}([C^{\text{SCFF}}] - [C^p])\big]^{-1}$$

and where v_{SCFF} and $\bar{v}_p$ are the volume fractions of the SCFF and polymer material, respectively, with respect to the volume of the RVE of the SFFRC. The elements of the Eshelby tensor $[S^{\text{SCFF}}]$ for the cylindrical SCFF reinforcement in the isotropic polymer matrix are given by [Qiu and Weng 1990]

$$[S^{\text{SCFF}}] = \begin{bmatrix} S_{1111} & S_{1122} & S_{1133} & 0 & 0 & 0 \\ S_{2211} & S_{2222} & S_{2233} & 0 & 0 & 0 \\ S_{3311} & S_{3322} & S_{3333} & 0 & 0 & 0 \\ 0 & 0 & 0 & S_{2323} & 0 & 0 \\ 0 & 0 & 0 & 0 & S_{1313} & 0 \\ 0 & 0 & 0 & 0 & 0 & S_{1212} \end{bmatrix}, \tag{19}$$

in which

$$S_{1111} = 0, \qquad S_{2222} = S_{3333} = \frac{5 - 4\nu^p}{8(1-\nu^p)}, \quad S_{2211} = S_{3311} = \frac{\nu^p}{2(1-\nu^p)},$$

$$S_{2233} = S_{3322} = \frac{4\nu^p - 1}{8(1-\nu^p)}, \quad S_{1122} = S_{1133} = 0, \qquad S_{1313} = S_{1212} = 1/4, \qquad S_{2323} = \frac{3 - 4\nu^p}{8(1-\nu^p)}.$$

Finally, the effective thermal expansion coefficient vector $\{\alpha\}$ of the SFFRC can be derived as [Laws 1973]

$$\{\alpha\} = \{\alpha^{\text{SCFF}}\} + ([C]^{-1} - [C^{\text{SCFF}}]^{-1})([C^{\text{SCFF}}]^{-1} - [C^p]^{-1})^{-1}(\{\alpha^{\text{SCFF}}\} - \{\alpha^p\}). \tag{20}$$

4. Results and discussion

In order to verify the validity of the MT model derived herein, the predictions of the MT model are first compared with the existing experimental and numerical results. Then the effective thermoelastic properties of the SFFRC containing wavy CNTs are determined by employing the MT model.

4.1. ***Comparison with experimental and numerical results.*** Recently, Kulkarni et al. [2010] experimentally and numerically investigated the elastic response of a nanoreinforced laminated composite (NRLC). The NRLC is made of CNT-reinforced polymer nanocomposite and carbon fiber. The cross sections of such NRLC are schematically shown in Figure 8. The geometry of the NRLC shown in Figure 8 is similar to that of the SCFF shown in Figure 3 if straight CNTs are considered. Thus, to confirm the modeling of the SCFF in the present study, we compare the results predicted by Kulkarni et al. [2010] for the NRLC with those predicted by the MT model for the SCFF with straight CNTs. It may be observed from Table 1 that the predicted value of the transverse Young's modulus (E_x) of the SCFF computed by the MT model matches closely with that of the experimental value predicted by Kulkarni et al. [2010]. The experimental value of E_x is lower than the theoretical prediction; this may be attributed to the fact that CNTs are not perfectly radially grown and straight, and hence the radial stiffening of the NRLC decreases [ibid.]. Further possible reasons for the disparity between the analytical and experimental results include lattice defects within CNTs [Ivanov et al. 2006; Yu et al. 2006] and the formation of voids in CNT-reinforced composites [Grunlan et al. 2006; Borca-Tasciuc et al. 2007]. Also, the value of E_x predicted by the MT model utilized herein is much closer to the experimental value than that of the numerical value predicted by Kulkarni et al. [2010]. This is attributed to the fact that the appropriate transformation and homogenization procedures given by (9) and (10) have been employed in the present study, whereas they did not consider such transformation and homogenization procedures in their numerical modeling. These comparisons are significant since the prediction of the transverse Young's modulus of the SCFF provides a critical check on the validity of the MT model. Thus it can be inferred from the comparisons shown in Table 1 that the MT model can be reasonably applied to predict the elastic properties of the SFFRC and its phases.

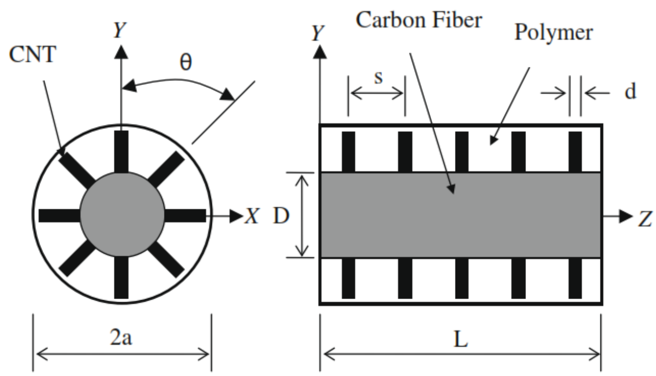

Figure 8. Transverse and longitudinal cross sections of the NRLC (adapted with permission from [Kulkarni et al. 2010]).

	NRLC*		
	Numerical*	Experimental*	MT model
E_x (GPa)	13.93	10.02	11.91
ν_{xy}	0.34	–	0.38
ν_{zx}	0.16	–	0.18

Table 1. Comparisons of the effective engineering constants of NRLC, 2% CNT and 41% IM7 carbon fiber, with those of SCFF containing straight CNTs. E_x is the transverse Young's modulus of the NRLC, ν_{zx} and ν_{xy} are the axial and transverse Poisson's ratios of the NRLC, respectively, and * indicates data from [Kulkarni et al. 2010].

	E_{yy} (GPa)		E_{xx} (GPa)	
$w = A/\lambda$	FE Model#	MT	FE Model#	MT
0	18	17.800	4.577	4.448
0.005	17.920	17.790	4.574	4.448
0.010	17.780	17.800	4.570	4.446
0.015	17.690	17.750	4.566	4.445
0.020	17.570	17.720	4.563	4.442
0.025	17.480	17.680	4.561	4.440
0.030	17.130	17.630	4.559	4.435

Table 2. Comparisons of the engineering constants of unwound PMNC material with sinusoidally wavy CNTs, where # indicates data from [Farsadi et al. 2013], with $E^n = 1030\,\text{GPa}$, $\nu^n = 0.063$, $E^p = 3.8\,\text{GPa}$, $\nu^p = 0.4$, and CNT volume fraction $v_n = 0.014$; w is the waviness ratio, A and λ are the amplitude and the wavelength of the sinusoidally wavy CNT, E^n and E^p are the Young's moduli of the CNT and polymer matrix, respectively, E_{yy} and E_{xx} are the axial and transverse Young's moduli of unwound PMNC containing sinusoidally wavy CNTs, respectively, and ν^n and ν^p are the Poisson's ratios of the CNT and polymer matrix, respectively.

Next, the engineering constants of unwound PMNC containing sinusoidally wavy CNTs determined by the MT model are compared with those of the similar nanocomposite containing sinusoidally wavy CNTs studied by Farsadi et al. [2013]. Table 2 illustrates these comparisons. The two sets of results predicted by the FE and MT models are in excellent agreement, validating the MT model used in this study. The CTEs of unwound PMNC containing straight CNTs determined by the MT model are also compared with those of the similar CNT-reinforced composite studied by Kirtania and Chakraborty [2009], as shown in Table 3. For the effective values of CTEs of the CNT-reinforced composite, the two sets of results predicted by the FE and MT models are in excellent agreement, validating the MT model used here. It may also be observed from Tables 2 and 3 that the analytical MT model presented in this study requires much less computational time than the FE model. Thus one may use the analytical MT model for intuitive predictions of the effective thermoelastic properties of any novel advanced composites.

	$\alpha_1(\times 10^{-6}\,\mathrm{K}^{-1})$		$\alpha_2(\times 10^{-6}\,\mathrm{K}^{-1})$	
v_n	FE Model$^{\$}$	MT	FE Model$^{\$}$	MT
0.5	25.2030	24.4850	69.7540	69.9030
1	15.3020	15.0720	72.8670	72.8790
3	5.0978	5.1820	74.7155	74.5120
5.45	2.2670	2.2978	73.5434	73.1220
7.9	1.0643	1.1170	71.7165	71.1300
10.3	0.4253	0.4847	69.7879	69.0140
15.77	−0.3201	−0.2560	65.1728	64.0370

Table 3. Comparisons of the CTEs of unwound PMNC material with straight CNTs, where $^{\$}$ indicates data from [Kirtania and Chakraborty 2009], with $E^n = 1000\,\mathrm{GPa}$, $\nu^n = 0.2$, $E^p = 3.89\,\mathrm{GPa}$, $\nu^p = 0.37$, $\alpha^n = -1.5 \times 10^{-6}\,\mathrm{K}^{-1}$, and $\alpha^p = 58 \times 10^{-6}\,\mathrm{K}^{-1}$; α_1 and α_2 are the axial and transverse CTEs of unwound PMNC with straight CNTs, respectively, and α^n and α^p are the CTEs of the CNT and polymer matrix, respectively.

4.2. ***Analytical modeling results.*** Armchair SWCNTs, carbon fiber, and polymer matrices are considered for evaluating the numerical results. Their material properties are taken from [Villeneuve et al. 1993; Peters 1998; Honjo 2007; Kwon et al. 2004; Shen and Li 2004] and are listed in Table 4. Since the investigations of earlier researchers [Yosida 2000; Maniwa et al. 2001; Jiang et al. 2004; Kwon et al. 2004; Jiang et al. 2009] have shown strong temperature dependence in the CTEs of CNTs, the variation in CTEs of the armchair (10, 10) CNT with temperature deviation is considered here. However, the elastic properties of CNTs, carbon fiber, and polymer are reported to be marginally dependent on the temperature deviation [Shen 2001]. Hence, the temperature dependence of the elastic properties of the constituent phases of the SFFRC is neglected. The relationships between the axial (α_3^n) and transverse (α_1^n) CTEs of the armchair (10, 10) CNT and the temperature deviation (ΔT) are given by [Kwon et al. 2004]:

$$\alpha_1^n = \alpha_2^n = 3.7601 \times 10^{-10}\Delta T^2 - 3.2189 \times 10^{-7}\Delta T - 3.2429 \times 10^{-8}\,\mathrm{K}^{-1}, \tag{21}$$

$$\alpha_3^n = 6.4851 \times 10^{-11}\Delta T^2 - 5.8038 \times 10^{-8}\Delta T + 9.0295 \times 10^{-8}\,\mathrm{K}^{-1}. \tag{22}$$

For the SFFRC, the hexagonal packing array of the SCFFs is considered for evaluating the numerical results. The maximum value of the CNT volume fraction in the SFFRC can be determined based on the

Material	C_{11}	C_{12}	C_{13}	C_{23}	C_{33}	C_{66}	α_1	α_2	
(10, 10) CNT[a]	288	254	87.8	87.8	1088	17	[b]	[b]	$d_n = 0.00136$
Carbon fiber[c,d]	236.4	10.6	10.6	10.7	24.8	25	1.1	6.8	$2a = 10$
Polymer[e]	4.09	1.55	1.55	1.55	4.09	1.27	66	66	

Table 4. Material properties of the constituent phases of the SFFRC, where [a] indicates data from [Shen and Li 2004], [c] [Honjo 2007], [d] [Villeneuve et al. 1993], and [e] [Peters 1998]. The values of α_1 and α_2 of the armchair (10, 10) CNT marked with [b] are from [Kwon et al. 2004] and are given in the text. Values of C are in units of GPa, α in $10^{-6}\,\mathrm{K}^{-1}$, and d_n and a in μm.

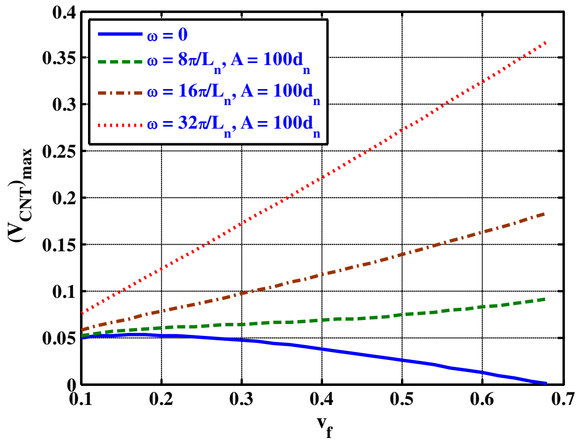

Figure 9. Variation of the maximum CNT volume fraction with the carbon fiber volume fraction in the SFFRC.

surface to surface distance at the roots of the two adjacent CNTs (0.0017 μm), the CNT diameter (d_n), and the running length of the sinusoidally wavy CNT (L_{nr}) as [Kundalwal and Ray 2013]

$$(V_{\text{CNT}})_{\max} = \frac{\pi d_n^2 L_{nr}}{d(d_n + 0.0017)^2} v_f, \tag{23}$$

where d_n is the diameter of the CNT in μm. The derivation of (23) can be found in [Kundalwal and Ray 2013]. It is evident from (2) and (23) that an increase in the amplitude of the CNT increases the running length of the CNT which eventually increases the maximum CNT volume fraction $(V_{\text{CNT}})_{\max}$ in the SFFRC. Figure 9 illustrates the variation of the maximum value of the CNT volume fraction in the SFFRC with the carbon fiber volume fraction (v_f) while the values of the wave frequency (ω) vary from $\omega = 8\pi/L_n$ to $\omega = 32\pi/L_n$. As expected, the maximum value of the CNT volume fraction in the SFFRC increases with the increase in the values of v_f and ω. To investigate the effect of wavy CNTs on the thermoelastic properties of the SFFRC, the value of ω is varied while keeping the value of v_f as 0.3, and adopting the following values of the other geometrical parameters of the RVE of the SFFRC:

- diameter of the armchair (10, 10) SWCNT $d_n = 0.00136\,\mu$m [Shen and Li 2004],
- radius of the carbon fiber $a = 5\,\mu$m,
- radius of the RVE of the SFFRC $R = 8.2888\,\mu$m,
- radius of the SCFF $b = 7.5353\,\mu$m,
- half-length of the carbon fiber $L_f = 100\,\mu$m,
- half-length of the RVE of the SFFRC $L = 110\,\mu$m,
- length of the straight CNT $L_n = 2.5353\,\mu$m,
- maximum amplitude of the wavy CNT $A = 100 d_n\,\mu$m,
- maximum waviness factor $A/L_n = 0.0536\,\mu$m.

First, the effective thermoelastic coefficients of the PMNC for different values of ω of the CNT are computed by employing the MT model. The estimated effective thermoelastic properties of the PMNC are then used to compute the effective thermoelastic properties of a SCFF in which the carbon fiber is the reinforcement and the matrix phase is the PMNC material. However, for the sake of brevity, the effective thermoelastic properties of the PMNC and SCFF are not presented here. Unless otherwise mentioned, the two fixed values of ω ($\omega = 16\pi/L_n$ and $\omega = 32\pi/L_n$) are considered for evaluating the results.

Figure 10 illustrates the variation of the effective elastic coefficients C_{11} and C_{12} of the SFFRC with waviness factor A/L_n. It may be observed from Figure 10(a) that the effective values of C_{11} of the SFFRC are not affected by variations of the amplitude of the wavy CNTs in the 2-3 plane. When the wavy CNTs are coplanar with the 1-3 plane, increase in the values of A/L_n and ω significantly increases C_{11}. Figure 10(b) reveals that the waviness of the CNTs causes a significant increase in the value of C_{12} when the wavy CNTs are coplanar with the 1-3 plane. Figure 11 demonstrates the variation of the values of C_{13} and C_{55} of the SFFRC with the waviness factor. Since the SFFRC is transversely isotropic material, the values of C_{13} are found to be identical to those of C_{12}, as shown in Figures 10(b)

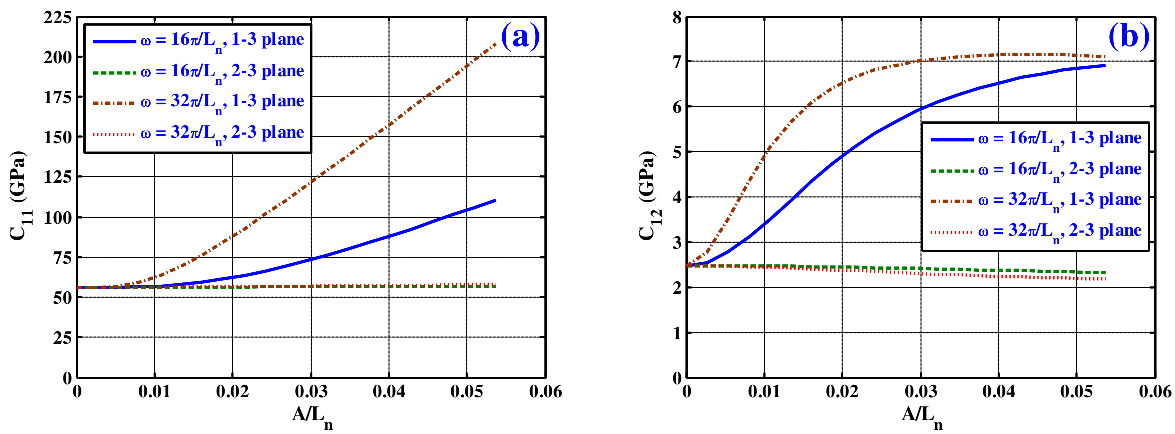

Figure 10. Variation of the effective elastic coefficients (a) C_{11} and (b) C_{12} of the SF-FRC with waviness factor ($v_f = 0.3$, $(V_{\mathrm{CNT}})_{\max}$).

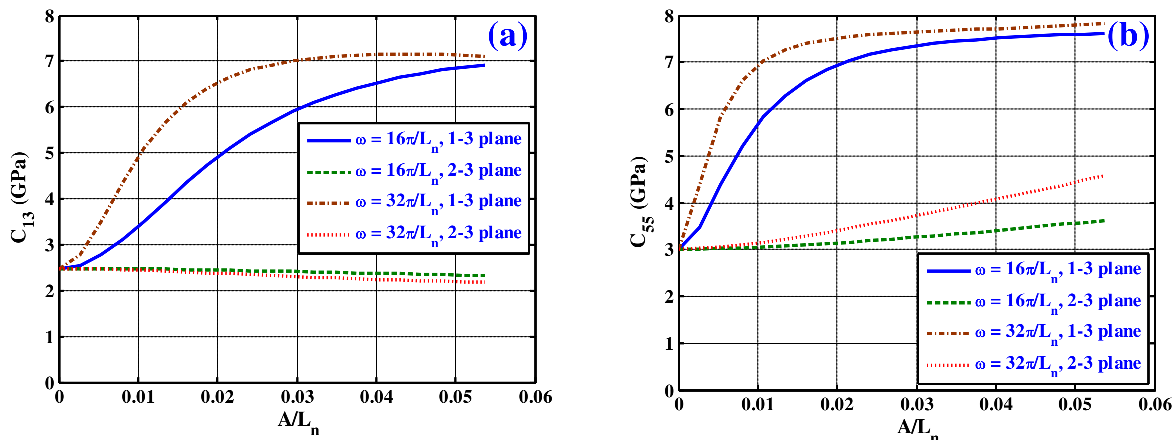

Figure 11. Variation of the effective elastic coefficients (a) C_{13} and (b) C_{55} of the SF-FRC with waviness factor ($v_f = 0.3$, $(V_{\mathrm{CNT}})_{\max}$).

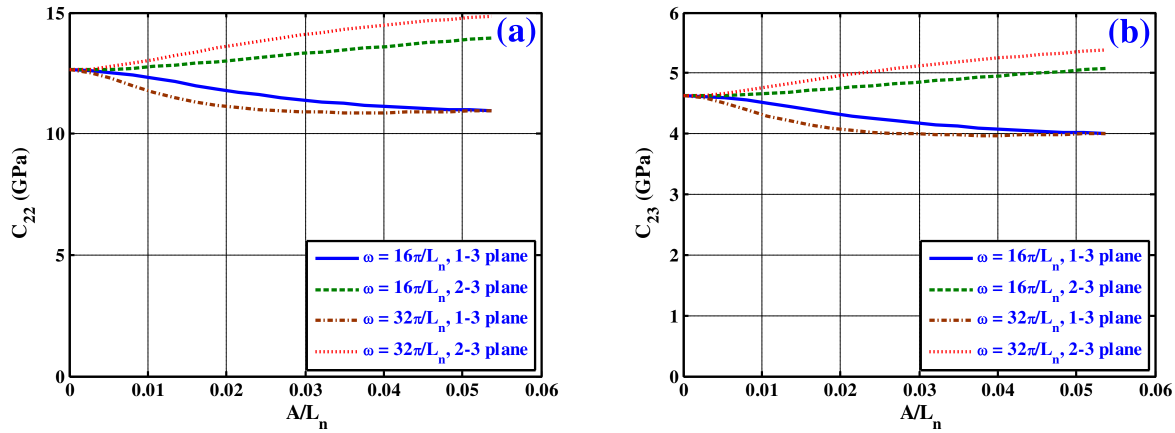

Figure 12. Variation of the effective elastic coefficients (a) C_{22} and (b) C_{23} of the SFFRC with waviness factor ($v_f = 0.3$, $(V_{\mathrm{CNT}})_{\max}$).

and 11(a). It may be observed from Figure 11(b) that the value of C_{55} of the SFFRC initially increases significantly, and then stabilizes for higher values of A/L_n, when the wavy CNTs are coplanar with the 1-3 plane. Figure 12(a) reveals that increase in the value of A/L_n decreases C_{22} when the CNT waviness is coplanar with the 1-3 plane, whereas the value of C_{22} increases for higher values of A/L_n when the CNT waviness is coplanar with the 2-3 plane. A similar trend is obtained for the value of C_{23}, as shown in Figure 12(b). Although not presented here, the same is true for the effective elastic coefficient C_{44}.

It may be noted from Figures 10–12 that if the wavy CNTs are coplanar with the 1-3 plane then the axial elastic coefficients of the SFFRC are significantly improved over their values with straight CNTs ($\omega = 0$) for higher values of A/L_n and ω. When the wavy CNTs are coplanar with the longitudinal plane (1-3 or $1'$-$3'$ plane) of the carbon fiber, as shown in Figure 2, the amplitudes of the CNT waves becomes parallel to the 1-axis, which results in the aligning of the projections of parts of the CNT lengths with the 1-axis leading to axial stiffening of the PMNC. The greater the value of ω, the more such projections will occur, and hence the effective axial elastic coefficients (C_{11}, C_{12}, C_{13}, C_{55}, and C_{66}) of the SFFRC increase with an increase in the value of ω. On the other hand, if the wavy CNTs are coplanar with the transverse plane (2-3 or $2'$-$3'$ plane) of the carbon fiber, then the transverse elastic coefficients (C_{22}, C_{23}, C_{33}, and C_{44}) of the SFFRC increase from their values with straight CNTs ($\omega = 0$). The reverse is true when the wavy CNTs are coplanar with the 1-3 ($1'$-$3'$) plane.

Figure 13 illustrates the variation in the axial (α_1) and transverse (α_2) CTEs of the SFFRC with the waviness factor. It may be observed from Figure 13(a) that the values of α_1 of the SFFRC are not affected by variations in the amplitude of the wavy CNTs in the 2-3 plane, whereas the value of α_1 initially increases and then significantly decreases for higher values of A/L_n and ω when the CNT waviness is coplanar with the 1-3 plane. It is also important to note from Figure 13(a) that the effective value of α_1 is zero for A/L_n and ω as 0.037 and $32\pi/L_n$, respectively, when the wavy CNTs are coplanar with the 1-3 plane. Figure 13(b) reveals that the waviness of the CNTs improves the effective values α_2 of the SFFRC when the wavy CNTs are coplanar with the 2-3 plane, compared to those of the SFFRC with straight CNTs ($\omega = 0$). Although not presented here, the computed effective values of α_3 are found to match identically with those of α_2, corroborating the fact that the SFFRC is transversely isotropic material.

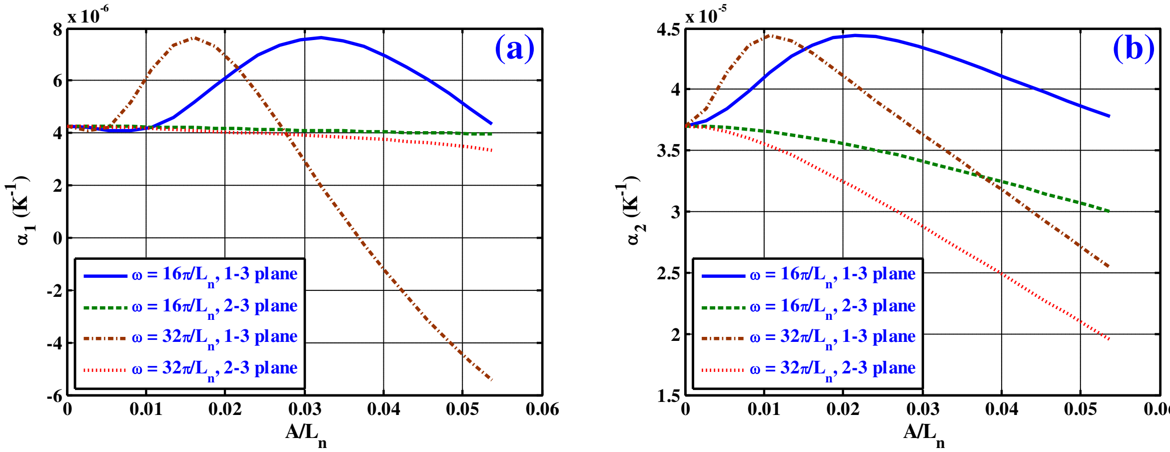

Figure 13. Variation of the effective (a) axial (α_1) and (b) transverse (α_2) CTEs of the FFRC with waviness factor ($\Delta T = 300\,K$, $v_f = 0.3$, $(V_{\mathrm{CNT}})_{\max}$).

Note from (20) that the CTEs of the SFFRC are dependent on the elastic coefficients of the SFFRC. Hence, with the increase in the value of A/L_n up to ~ 0.013, the axial elastic coefficients of the unwound PMNC are increased which eventually influences the effective CTEs of the unwound PMNC when the CNT waviness is coplanar with the 1-3 plane. Therefore, the effective CTEs (α_1, α_2, and α_3) of the FFRC are initially increased for lower values of A/L_n. For $A/L_n \geq 0.013$, the effective CTEs (α_1, α_2, and α_3) of the SFFRC with wavy CNTs coplanar with the 1-3 plane start to decrease. This is attributed to the fact that the negative axial and transverse CTEs (α_1^n and α_3^n) of the radially grown wavy CNTs on the circumferential surfaces of the carbon fibers significantly suppress the positive CTE ($\alpha^p = 66 \times 10^{-6}\,\mathrm{K}^{-1}$) of the polymer matrix, which eventually lowers the effective values of α_1 of the SFFRC. This effect becomes more pronounced for higher values of A/L_n and ω because the CNT volume fraction in the SFFRC increases with A/L_n and ω, as depicted in Figure 9. From Figures 10–13 it is important to note that the axial thermoelastic coefficients significantly improve for higher values of A/L_n and ω when the CNT waviness is coplanar with the 1-3 plane. The effect of wavy CNTs coplanar with the 2-3 plane on the axial thermoelastic coefficients of the SFFRC is not as pronounced. On the other hand, marginal improvement in the transverse thermoelastic coefficients of the SFFRC is observed when the CNT waviness is coplanar with the 2-3 plane. Hence, for investigating the effect of temperature deviation on the effective thermal expansion coefficients of the SFFRC, the wavy CNTs are considered to be coplanar with the 1-3 plane when the values of ω and A are $32\pi/L_n$ and $0.136\,\mu$m, respectively.

Practically, the carbon fiber volume fraction in short fiber composites can vary, typically from 0.2 to 0.6. Hence, to analyze the effect of temperature deviation on the effective thermal expansion coefficients of the SFFRC, the two discrete values of the carbon fiber volume fraction are considered, 0.25 and 0.55. Figure 14(a) and (b) illustrate the variation of the values of α_1 and α_2 of the SFFRC, respectively, with the temperature deviation for different values of the carbon fiber volume fraction. It is important to note from these figures that the effective values of CTEs of the SFFRC decrease with the increase in the temperature deviation for higher values of v_f and ω. It may also be observed that wavy CNTs coplanar with the 1-3 plane significantly improve the CTEs of the SFFRC over the values with straight CNTs

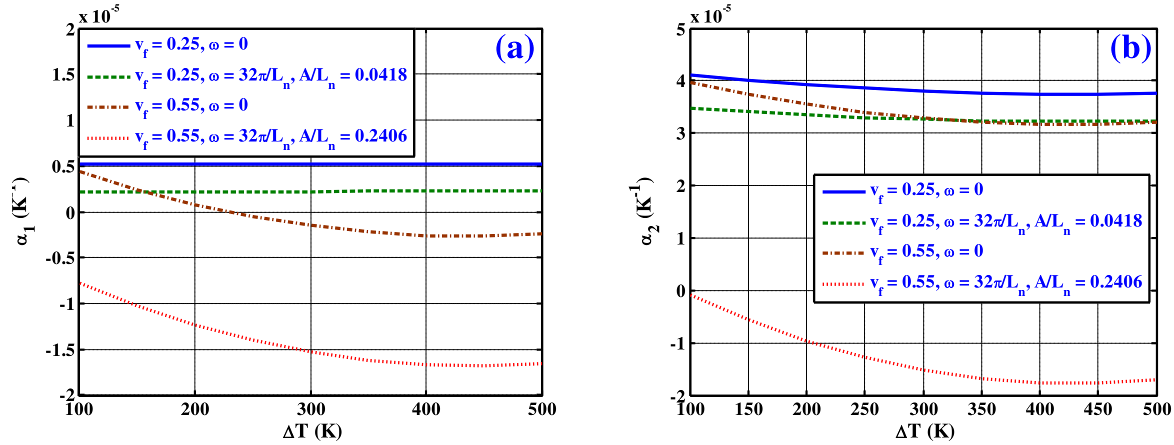

Figure 14. Variation of the effective (a) axial (α_1) and (b) transverse (α_2) CTEs of the SFFRC with temperature deviation when the wavy CNTs are coplanar with the longitudinal plane (that is, 1-3 plane) of the carbon fiber ($A = 0.136\,\mu$m).

($\omega = 0$). This is attributed to the fact that as the values of v_f and ω increase the CNT volume fraction in the SFFRC increases, as shown in Figure 9, which eventually improves the values of the CTEs of the SFFRC. It is also seen from these two plots that the CTEs of the SFFRC can be modified by changing the values of A/L_n and ω according to the requirements of thermal management.

5. Conclusions

The effective thermoelastic properties of a novel short fuzzy fiber-reinforced composite (SFFRC) containing wavy carbon nanotubes (CNTs) have been investigated. An analytical micromechanics model based on the Mori–Tanaka model was utilized to predict the effective thermoelastic coefficients of this novel composite. The influence of the waviness of the CNTs on the thermoelastic coefficients of the SFFRC has been studied, considering sinusoidally wavy CNTs to be coplanar with either of two mutually orthogonal planes. The following main conclusions can be drawn from the investigations carried out here.

(1) If the plane of the radially grown wavy CNTs is coplanar with the longitudinal plane of the carbon fiber then the axial effective thermoelastic coefficients of the SFFRC are significantly improved over those of the FFRC with either straight CNTs ($\omega = 0$) or wavy CNTs coplanar with the transverse plane of the carbon fiber.

(2) When the CNT waviness is coplanar with the transverse plane of the carbon fiber, marginal improvement has been observed in the transverse effective thermoelastic coefficients of the SFFRC.

(3) If the CNT waviness is coplanar with the longitudinal plane of the carbon fiber then the thermoelastic response of the SFFRC significantly improves with an increase in the temperature for higher values of the carbon fiber volume fraction, waviness factor, and wave frequency of the CNT.

Therefore, the SFFRC with sinusoidally wavy CNTs studied here may be used for advanced structures that require stringent constraints on dimensional stability.

List of abbreviations

CNT	Carbon nanotube
CTE	Coefficient of thermal expansion
CVD	Chemical vapor deposition
FE	Finite element
MDS	Molecular dynamics simulation
MT	Mori–Tanaka
MWCNT	Multiwalled carbon nanotube
NRLC	Nanoreinforced laminated composite
PMNC	Polymer matrix nanocomposite
RVE	Representative volume element
SCFF	Short composite fuzzy fiber
SEM	Scanning electron microscopy
SFFRC	Short fuzzy fiber-reinforced composite
SWCNT	Single-walled carbon nanotube

List of symbols

A	Amplitude of the CNT (μm)
$[\tilde{A}_1]$, $[\tilde{A}_2]$, $[\tilde{A}_3]$	Matrices of the strain concentration factors
a	Radius of the carbon fiber (μm)
b	Radius of the SCFF (μm)
$[\bar{C}^{\mathrm{NC}}]$	Elastic coefficient matrix of the unwound PMNC containing wavy CNTs (GPa)
$[C^r]$	Elastic coefficient matrix of the r-th phase (GPa)
C_{ij}^r	Elastic coefficients of the r-th phase (GPa)
d_n	Diameter of the CNT (μm)
E^n and E^p	Young's moduli of the CNT and polymer matrix, respectively (GPa)
E_x	Transverse Young's modulus of the NRLC (GPa)
E_{yy} and E_{xx}	Axial and transverse Young's moduli of the unwound PMNC containing sinusoidally wavy CNTs, respectively (GPa)
$[I]$	Fourth-order identity matrix
L	Length of the RVE of the SFFRC (μm)
L_f	Half-length of the short carbon fiber embedded in the RVE of the SFFRC (μm)
L_n	Length of straight CNT (μm)
L_{nr}	Running length of sinusoidally wavy CNT (μm)
$(N_{\mathrm{CNT}})_{\max}$	Maximum number of radially grown aligned CNTs on the circumferential surface of the short carbon fiber
n	Number of waves of a sinusoidally wavy CNT along its axial direction
R	Radius of the RVE of the SFFRC (μm)
$[S^r]$	Eshelby tensor of the r-th domain
S_{ij}^r	Elements of the Eshelby tensor of the r-th domain
$[T]$, $[T_1]$, $[T_2]$	Transformation matrices
$(V_{\mathrm{CNT}})_{\max}$	Maximum volume fraction of the CNT in the SFFRC
v_{SCFF}	Volume fraction of the SCFF in the SFFRC
v_f	Volume fraction of the carbon fiber in the SFFRC
$\bar{v}_f$	Volume fraction of the carbon fiber in the SCFF
v_m	Volume fraction of the matrix in the composite
v_n	Volume fraction of the CNT in the PMNC/the CNT-reinforced nanocomposite

v_{PMNC}	Volume fraction of the PMNC in the SCFF
v_P	Volume fraction of the polymer in the PMNC
$\bar{v}_P$	Volume fraction of the polymer in the SFFRC
v_{SCFF}	Volume fraction of the SCFF in the SFFRC
$\{\alpha\}$	Thermal expansion coefficient vector of the SFFRC (K^{-1})
$\{\alpha^r\}$	Thermal expansion coefficient vector of the r-th phase (K^{-1})
α_i^r	Thermal expansion coefficients of the r-th phase (K^{-1})
ΔT	Temperature deviation from the reference temperature (K)
$\{\epsilon^r\}$	Strain vector of the r-th phase
λ	Wavelength of the CNT (nm)
ν^n and ν^p	Poisson's ratios of the CNT and polymer matrix, respectively
ν_{zx} and ν_{xy}	Axial and transverse Poisson's ratios of the unwound PMNC containing sinusoidally wavy CNTs, respectively
$\{\sigma^r\}$	Stress vector of the r-th phase (GPa)
ω	Wave frequency of the CNT ($\mu\mathrm{m}^{-1}$)

References

[Ajayan and Tour 2007] P. M. Ajayan and J. M. Tour, "Material science: nanotube composites", *Nature* **447** (2007), 1066–1068.

[Alamusi et al. 2012] Alamusi, N. Hu, B. Jia, M. Arai, C. Yan, J. Li, Y. Liu, S. Atobe, and H. Fukunaga, "Prediction of thermal expansion properties of carbon nanotubes using molecular dynamics simulations", **54** (2012), 249–254.

[Anumandla and Gibson 2006] V. Anumandla and R. F. Gibson, "A comprehensive closed form micromechanics model for estimating the elastic modulus of nanotube-reinforced composites", *Composites Part A: Applied Science and Manufacturing* **37**:12 (2006), 2178–2185.

[Ashrafi and Hubert 2006] B. Ashrafi and P. Hubert, "Modeling the elastic properties of carbon nanotube array/polymer composites", *Composites Science and Technology* **66**:3–4 (2006), 387–396.

[Bandow 1997] S. Bandow, "Radial thermal expansion of purified multiwall carbon nanotubes measured by X-ray diffraction", *Japanese Journal of Applied Physics* **36** (1997), L1403–L1405.

[Benveniste 1987] Y. Benveniste, "A new approach to the application of Mori-Tanaka's theory in composite materials", *Mechanics of Materials* **6**:2 (1987), 147–157.

[Berhan et al. 2004] L. Berhan, Y. B. Yi, and A. M. Sastry, "Effect of nanorope waviness on the effective moduli of nanotube sheets", *Journal of Applied Physics* **95**:9 (2004), 5027–5034.

[Borca-Tasciuc et al. 2007] T. Borca-Tasciuc, M. Mazumdar, Y. Son, S. K. Pal, L. S. Schadler, and P. M. Ajayan, "Anisotropic thermal diffusivity characterization of aligned-carbon nanotube-polymer composites", *Journal of Nanoscience and Nanotechnology* **7**:4–5 (2007), 1581–1588.

[Bower et al. 2000] C. Bower, W. Zhu, S. Jin, and O. Zhou, "Plasma-induced alignment of carbon nanotubes", *Applied Physics Letters* **77**:6 (2000), 830–832.

[Chatzigeorgiou et al. 2012] G. Chatzigeorgiou, Y. Efendiev, N. Charalambakis, and D. C. Lagoudas, "Effective thermoelastic properties of composites with periodicity in cylindrical coordinates", *International Journal of Solids and Structures* **49**:18 (2012), 2590–2603.

[Esteva and Spanos 2009] M. Esteva and P. D. Spanos, "Effective elastic properties of nanotube reinforced composites with slightly weakened interfaces", *Journal of Mechanics of Materials and Structures* **4**:5 (2009), 887–900.

[Farsadi et al. 2013] M. Farsadi, A. Öchsner, and M. Rahmandoust, "Numerical investigation of composite materials reinforced with waved carbon nanotubes", *Journal of Composite Materials* **47**:11 (2013), 1425–1434.

[Fisher et al. 2002] F. T. Fisher, R. D. Bradshaw, and L. C. Brinson, "Effects of nanotube waviness on the modulus of nanotube-reinforced polymers", *Applied Physics Letters* **80**:24 (2002), 4647–4649.

[Garcia et al. 2008] E. J. Garcia, B. L. Wardle, A. J. Hart, and N. Yamamoto, "Fabrication and multifunctional properties of a hybrid laminate with aligned carbon nanotubes grown *In Situ*", *Composites Science and Technology* **68**:9 (2008), 2034–2041.

[Grunlan et al. 2006] J. C. Grunlan, Y. Kim, S. Ziaee, X. Wei, B. Abdel-Magid, and K. Tao, "Thermal and mechanical behavior of carbon-nanotube-filled latex", *Macromolecular Material Engineering* **291**:9 (2006), 1035–1043.

[Honjo 2007] K. Honjo, "Thermal stresses and effective properties calculated for fiber composites using actual cylindrically-anisotropic properties of interfacial carbon coating", *Carbon* **45**:4 (2007), 865–872.

[Hsiao and Daniel 1996] H. M. Hsiao and I. M. Daniel, "Elastic properties of composites with fiber waviness", *Composites Part A: Applied Science and Manufacturing* **27**:10 (1996), 931–941.

[Iijima 1991] S. Iijima, "Helical microtubules of graphitic carbon", *Nature* **354**:6348 (1991), 56–58.

[Ivanov et al. 2006] I. Ivanov, A. Puretzky, G. Eres, H. Wang, Z. Pan, H. Cui, R. Jin, J. Howe, and D. B. Geohegan, "Fast and highly anisotropic thermal transport through vertically aligned carbon nanotube arrays", *Applied Physics Letters* **89**:22 (2006), Article ID #223110.

[Jiang et al. 2004] H. Jiang, B. Liu, Y. Huang, and K. C. Hwang, "Thermal expansion of single wall carbon nanotubes", *ASME Journal of Engineering Materials and Technology* **126**:3 (2004), 265–270.

[Jiang et al. 2009] J.-W. Jiang, J.-S. Wang, and B. Li, "Thermal expansion in single-walled carbon nanotubes and graphene: nonequilibrium Green's function approach", *Phys. Rev. B* **80**:20 (2009), 205429.

[Khondaker and Keng 2012] S. A. Khondaker and A. K. Keng, "A pull-out model for perfectly bonded carbon nanotube in polymer composites", *Journal of Mechanics of Materials and Structures* **7**:8–9 (2012), 753–764.

[Kirtania and Chakraborty 2009] S. Kirtania and D. Chakraborty, "Evaluation of thermoelastic properties of carbon nanotube-based composites using finite element method", in *Proceedings of the International Conference on Mechanical Engineering AM-13*, Dhaka, Bangladesh, 2009.

[Kulkarni et al. 2010] M. Kulkarni, D. Carnahan, K. Kulkarni, D. Qian, and J. L. Abot, "Elatsic response of a carbon nanotube fiber reinforced polymeric composite: A numerical and experimental study", *Composites Part B: Engineering* **41**:5 (2010), 414–421.

[Kundalwal 2013] S. I. Kundalwal, *Micromechanical analysis of novel continuous and short fuzzy fiber reinforced composites*, Ph.D. thesis, Department of Mechanical Engineering, Indian Institute of Technology Kharagpur, 2013.

[Kundalwal and Ray 2012] S. I. Kundalwal and M. C. Ray, "Effective properties of a novel composite reinforced with short carbon fibers and radially aligned carbon nanotubes", *Mechanics of Materials* **53** (2012), 47–60.

[Kundalwal and Ray 2013] S. I. Kundalwal and M. C. Ray, "Effect of carbon nanotube waviness on the elastic properties of the fuzzy fiber reinforced composites", *ASME Journal of Applied Mechanics* **80**:2 (2013), 021010.

[Kwon et al. 2004] Y.-K. Kwon, S. Berber, and D. Tománek, "Thermal contraction of carbon fullerenes and nanotubes", *Physical Review Letters* **92**:1 (2004), 015901.

[Laws 1973] N. Laws, "On the thermostatics of composite materials", *Journal of the Mechanics and Physics of Solids* **21**:1 (1973), 9–17.

[Li and Chou 2009] C. Li and T.-W. Chou, "Failure of carbon nanotube/polymer composites and the effect of nanotube waviness", *Composites Part A: Applied Science and Manufacturing* **40**:10 (2009), 1580–1586.

[Li and Dunn 1998] J. Y. Li and M. L. Dunn, "Anisotropic coupled-field inclusion and inhomogeneity problems", *Philosophical Magazine A* **77**:5 (1998), 1341–1350.

[Li and Guo 2008] H. Li and W. Guo, "Transversely isotropic elastic properties of single-walled carbon nanotubes by a rectangular beam model for the C-C bonds", *Journal of Applied Physics* **103**:10 (2008), Article ID #103501.

[Liu et al. 2005] J. Z. Liu, Q.-S. Zheng, L.-F. Wang, and Q. Jiang, "Mechanical properties of single-walled carbon nanotube bundles as bulk materials", *Journal of the Mechanics and Physics of Solids* **53**:1 (2005), 123–142.

[Maniwa et al. 2001] Y. Maniwa, R. Fujiwara, H. Kira, H. Tou, H. Kataura, S. Suzuki, Y. Achiba, E. Nishibori, M. Takata, M. Sakata, A. Fujiwara, and H. Suematsu, "Thermal expansion of single-walled carbon nanotube (SWNT) bundles: X-ray diffraction studies", *Phys. Rev. B* **64**:24 (2001), 241402.

[Meguid et al. 2010] S. A. Meguid, J. M. Wernik, and Z. Q. Cheng, "Atomistic-based continuum representation of the effective properties of nano-reinforced epoxies", *International Journal of Solids and Structures* **47**:13 (2010), 1723–1736.

[Mori and Tanaka 1973] T. Mori and K. Tanaka, “Average stress in matrix and average elastic energy of materials with misfitting inclusions”, *Acta Metallurgica* **21**:5 (1973), 571–574.

[Natsuki et al. 2004] T. Natsuki, K. Tantrakarn, and M. Endo, “Prediction of elastic properties for single-walled carbon nanotubes”, *Carbon* **42**:1 (2004), 39–45.

[Odegard et al. 2003] G. M. Odegard, T. S. Gates, K. E. Wise, C. Park, and E. J. Siochi, “Constitutive modeling of nanotube-reinforced polymer composites”, *Composites Science and Technology* **63**:11 (2003), 1671–1687.

[Pantano and Cappello 2008] A. Pantano and F. Cappello, “Numerical model for composite material with polymer matrix reinforced by carbon nanotubes”, *Meccanica* **43**:2 (2008), 263–270.

[Peters 1998] S. T. Peters, *Handbook of Composites*, Chapman and Hall, London, 1998.

[Pipes and Hubert 2003] R. B. Pipes and P. Hubert, “Helical carbon nanotube arrays: thermal expansion”, *Composites Science and Technology* **63**:11 (2003), 1571–1579.

[Qian et al. 2000] D. Qian, E. C. Dickey, R. Andrews, and T. Rantell, “Load transfer and deformation mechanisms in carbon nanotube-polystyrene composites”, *Applied Physics Letters* **76**:20 (2000), 2868–2870.

[Qiu and Weng 1990] Y. P. Qiu and G. J. Weng, “On the application of Mori-Tanaka’s theory involving transversely isotropic spheroidal inclusions”, *Internat. J. Engrg. Sci.* **28**:11 (1990), 1121–1137.

[Qiu et al. 2007] J. Qiu, C. Zhang, B. Wang, and R. Liang, “Carbon nanotube integrated multifunctional multiscale composites”, *Nanotechnology* **18**:27 (2007), 275708.

[Raravikar et al. 2002] N. R. Raravikar, P. Keblinski, A. M. Rao, M. S.Dresselhaus, L. S. Schadler, and P. M. Ajayan, “Temperature dependence of radial breathing mode Raman frequency of single-walled carbon nanotubes”, *Phys. Rev. B* **66**:23 (2002), 235424.

[Ray and Batra 2009] M. C. Ray and R. C. Batra, “Effective properties of carbon nanotube and piezoelectric fiber reinforced hybrid smart composites”, *ASME Journal of Applied Mechanics* **76**:3 (2009), 034503.

[Schulte and Windle 2007] K. Schulte and A. H. Windle, “Editorial”, *Composites Science and Technology* **67**:5 (2007), 777.

[Seidel and Lagoudas 2006] G. D. Seidel and D. C. Lagoudas, “Micromechanical analysis of the effective elastic properties of carbon nanotube reinforced composites”, *Mechanics of Materials* **38**:8–10 (2006), 884–907.

[Shaffer and Windle 1999] M. S. P. Shaffer and A. H. Windle, “Fabrication and characterization of carbon nanotube/poly(vinyl alcohol) composites”, *Advanced Materials* **11**:11 (1999), 937–941.

[Shen 2001] H.-S. Shen, “Hygrothermal effects on the postbuckling of shear deformable laminated plates”, *International Journal of Mechanical Sciences* **43**:5 (2001), 1259–1281.

[Shen and Li 2004] L. Shen and J. Li, “Transversely isotropic elastic properties of single-walled carbon nanotubes”, *Physical Review B* **69**:4 (2004), 045414.

[Shi et al. 2004] D.-L. Shi, X.-Q. Feng, Y. Y. Huang, K.-C. Hwang, and H. Gao, “The effect of nanotube waviness and agglomeration on the elastic property of carbon nanotube-reinforced composites”, *ASME Journal of Engineering Materials and Technology* **126**:3 (2004), 250–257.

[Thostenson et al. 2001] E. T. Thostenson, Z. Ren, and T.-W. Chou, “Advances in the science and technology of carbon nanotubes and their composites: a review”, *Composites Science and Technology* **61**:13 (2001), 1899–1912.

[Treacy et al. 1996] M. M. J. Treacy, T. W. Ebbesen, and J. M. Gibson, “Exceptionally high Young’s modulus observed for individual carbon nanotubes”, *Nature* **381**:6584 (1996), 678–680.

[Tsai et al. 2011] C.-H. Tsai, C. Zhang, D. A. Jack, R. Liang, and B. Wang, “The effect of inclusion waviness and waviness distribution on elastic properties of fiber-reinforced composites”, *Composites Part B: Engineering* **42**:1 (2011), 62–70.

[Veedu et al. 2006] V. P. Veedu, A. Cao, X. Li, K. Ma, C. Soldano, S. Kar, P. M. Ajayan, and M. N. Ghasemi-Nejhad, “Multifunctional composites using reinforced laminae with carbon-nanotube forests”, *Nature Materials* **5**:6 (2006), 457–462.

[Villeneuve et al. 1993] J. F. Villeneuve, R. Naslain, R. Fourmeaux, and J. Sevely, “Longitudinal/radial thermal expansion and poisson ratio of some ceramic fibers as measured by transmission electron microscopy”, *Composites Science and Technology* **49**:1 (1993), 89–103.

[Yamamoto et al. 2009] N. Yamamoto, A. J. Hart, E. J. Garcia, S. S. Wicks, H. M. Duong, A. H. Slocum, and B. L. Wardle, "High-yield growth and morphology control of aligned carbon nanotubes on ceramic fibers for multifunctional enhancement of structural composites", *Carbon* **47**:3 (2009), 551–560.

[Yosida 2000] Y. Yosida, "High-temperature shrinkage of single-walled carbon nanotube bundles up to 1600 K", *Journal of Applied Physics* **87**:7 (2000), 3338–3341.

[Yu et al. 2006] A. Yu, M. E. Itkis, E. Bekyarova, and R. C. Haddon, "Effect of single-walled carbon nanotube purity on the thermal conductivity of carbon nanotube-based composites", *Applied Physics Letters* **89**:13 (2006), Article ID #133102.

[Zhang et al. 2008] Q. Zhang, J.-Q. Huang, M.-Q. Zhao, W.-Z. Qian, Y. Wang, and F. Wei, "Radial growth of vertically aligned carbon nanotube arrays from ethylene on ceramic spheres", *Carbon* **46**:8 (2008), 1152–1158.

Received 15 Mar 2013. Revised 27 Aug 2013. Accepted 27 Oct 2013.

SHAILESH I. KUNDALWAL: shail_kundal@yahoo.com
Department of Mechanical Engineering, Indian Institute of Technology, Kharagpur 721302, India

MANAS C. RAY: mcray@mech.iitkgp.ernet.in
Department of Mechanical Engineering, Indian Institute of Technology, Kharagpur 721302, India

JOURNAL OF MECHANICS OF MATERIALS AND STRUCTURES

msp.org/jomms

Founded by Charles R. Steele and Marie-Louise Steele

Cover photo: Ev Shafrir

See msp.org/jomms for submission guidelines.

JoMMS (ISSN 1559-3959) at Mathematical Sciences Publishers, 798 Evans Hall #6840, c/o University of California, Berkeley, CA 94720-3840, is published in 10 issues a year. The subscription price for 2014 is US $555/year for the electronic version, and $710/year (+$60, if shipping outside the US) for print and electronic. Subscriptions, requests for back issues, and changes of address should be sent to MSP.

JoMMS peer-review and production is managed by EditFlow® from Mathematical Sciences Publishers.

PUBLISHED BY

mathematical sciences publishers

nonprofit scientific publishing

http://msp.org/

Journal of Mechanics of Materials and Structures

Volume 9, No. 1 January 2014

Improved thermoelastic coefficients of a novel short fuzzy fiber-reinforced composite with wavy carbon nanotubes
SHAILESH I. KUNDALWAL and MANAS C. RAY 1

Moment Lyapunov exponents and stochastic stability of coupled viscoelastic systems driven by white noise
JIAN DENG, WEI-CHAU XIE and MAHESH D. PANDEY 27

Combined effects of interstitial and Laplace pressure in hot isostatic pressing of cylindrical specimens LAURA GALUPPI and LUCA DESERI 51

Planar grained structures with traction-smoothing inclusions: an elastostatic numerical analysis for shear and torsion SHMUEL VIGDERGAUZ 87

Continuous contact problem for two elastic layers resting on an elastic half-infinite plane ERDAL ÖNER and AHMET BIRINCI 105

1559-3959(2014)9:1;1-9